JOURNAL OF COMPUTATIONAL PHYSICS 27, 397–409 (1978)

A Finite-Particle Scheme for Three-Dimensional Gas Dynamics

RICHARD B. LARSON

Department of Astronomy, Yale University, New Haven, Connecticut 06520

Received May 5, 1977

A method for simulating three-dimensional gas dynamics by following the motions of representative fluid particles is described. The gas pressure is represented by repulsive forces between neighboring pairs of particles, and the effect of shock dissipation is represented by an artificial-viscosity force between neighboring particles. Tests show that the scheme represents the static pressure and the oscillation period of an enclosed gas sphere with an accuracy of ≈ 5 % for 100 particles, and it reproduces the Jeans criterion for spherical gravitational collapse with an accuracy of ≈ 20 %. It also simulates the formation of accretion discs as thin as ~ 10 percent of the diameter, with an effective Reynolds number due to artificial viscosity of $\mathscr{R} \approx 50$.

1. INTRODUCTION

Many problems in astrophysical gas dynamics are inherently three-dimensional in nature, involving systems with no special symmetries. One such problem is the gravitational collapse of interstellar clouds and the formation of stars. Previous calculations assuming spherical or axial symmetry have shown that collapsing clouds always tend to develop highly condensed cores or "condensation nuclei" of stellar density, which subsequently grow in mass by the accretion of remnant cloud material [1]. In the more realistic case where no symmetries are present, a collapsing cloud probably develops many condensation centers orbiting around each other and continuing to accrete from the surrounding cloud. A question of vital interest concerns the number and the mass distribution of the protostellar condensations that form in a collapsing cloud.

At present, three-dimensional calculations with standard Eulerian or Lagrangian methods are feasible only with fairly coarse grids containing, perhaps, 32^3 cells. For an Eulerian scheme with a fixed grid, this spatial resolution is not adequate to follow very far the development of small dense condensations in a collapsing cloud. Nor is the Eulerian method well suited to following accurately the motions of such condensations, since numerical inaccuracies in the conservation of mass and momentum can lead to spurious numerical diffusion and viscosity effects. On the other hand, Lagrangian schemes which follow the fluid motion have the disadvantage that the cells quickly become highly distorted, necessitating frequent rezoning which is time consuming and itself introduces errors or disturbances into the calculation.

These limitations can be avoided and the development of arbitrarily small condensa-

0021-9991/78/0273–0397$02.00/0

tions can be followed if the use of a grid is abandoned altogether and one follows individually the motions of many representative fluid elements or particles, as in the many-body techniques used in molecular dynamics and in stellar dynamics. Such an approach is well suited to studying the formation and growth of small dense condensations, which are represented by close gravitationally bound clusterings of particles. This paper describes a finite-particle scheme which has been developed and used especially to study the gravitational fragmentation of collapsing gas clouds; some preliminary results of this work have already been reported [1], and more detailed results will be published elsewhere [14].

2. The Finite-Particle Method

(a) *The Representation of Pressure*

There are two ways in which the temperature and pressure of a gas can be represented in a finite-particle scheme. One approach is to treat the particles as giant molecules which interact only via collisions, but otherwise follow free particle orbits. The pressure then arises almost entirely from the random or "thermal" motions of the particles, and any radiative heating or cooling of the gas is represented by inelastic collisions. A scheme of this type in which the particles are inelastically colliding spheres has been described by Brahic [2, 3], who has used it to study the evolution of systems of solid particles such as Saturn's rings. A disadvantage of this approach for the present purposes is that it is necessary to give the particles an unphysical finite size which must be fairly large, or else inelastic collisions will be too infrequent to dissipate energy during a free-fall time as required in a collapsing cloud.

A second possibility is to regard the particles as extended but amorphous and deformable gas elements which are in continual contact with neighboring gas elements and interact with them via pressure forces at the boundaries. The pressure force between two neighboring gas elements then depends on the assumed temperature and on the separation between their centers. Consider for example two neighboring elements with separation r, mass m, radius $\sim r$, and density $\rho \sim m/r^3$ (Fig. 1). If the isothermal sound speed is c, the pressure within each element is $P = \rho c^2$ and the total repulsive force between them is PA, where $A \sim r^2$ is the area of the interface; the repulsive acceleration is then

$$a_r = \frac{PA}{m} \sim \frac{\rho c^2 r^2}{\rho r^3} = \frac{c^2}{r}. \tag{1}$$

Although this derivation is only approximate, any more exact result must have the same form as (1), which also gives the pressure acceleration between neighboring points in a Lagrangian grid. Therefore we have adopted a law of this form for the repulsive acceleration between neighboring particles:

$$a_r = \frac{C^2}{r} \tag{2}$$

where C is a parameter, proportional to the isothermal sound speed, whose exact relation to the total pressure is to be determined (see below). In the applications that have been made of this method the gas has been assumed to remain isothermal, so that C is a constant throughout the calculation.

Similar schemes, with a more artificial form for the pressure force, have been described by Dormand and Woolfson [4] and by Aust [5].

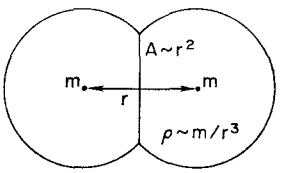

FIG. 1. Schematic representation of two adjacent gas elements, as visualized in estimating the pressure force between them.

(b) *The Representation of Viscosity*

The viscosity of a gas plays a somewhat analogous role to the pressure in that, while pressure tends to smooth out density fluctuations, viscosity tends to smooth out velocity fluctuations and dissipate their energy. The presence of viscous dissipation is crucial for the formation of stars in a collapsing cloud, since it is needed to dissipate the kinetic energy of collapse. The fact that molecular viscosity is small does not mean that its effects are unimportant, but rather that they are confined to thin regions of almost discontinuous velocity change, i.e. to shock fronts. For example, in the existing spherical collapse models, nearly all of the dissipation takes place in an accretion shock at the surface of a stellar core. If the collapse motions are more irregular, shock fronts may also play an important role in transferring momentum from one part of the cloud to another, thus providing an effective large-scale viscosity and contributing to the redistribution of angular momentum which is also essential for the formation of stars [1]. For these reasons it is important to include the effect of shock fronts in providing dissipation and an effective large-scale viscosity.

The average rate of momentum transfer between adjacent fluid elements due to the propagation of shock fronts may be estimated as follows. Consider two representative fluid particles with separation r that are approaching each other with relative velocity u (Fig. 2). If u is comparable with or greater than the sound speed, then a shock front must appear somewhere between the particles and propagate toward one of them, overtaking it in a time $\sim r/u$ and imparting to it a velocity increment $\sim u$ away from the other particle. Although the detailed properties of such shocks cannot be determined,

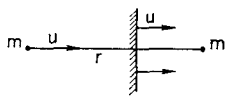

FIG. 2. Sketch illustrating the possible configuration of two approaching particles and a shock front propagating between them.

the average acceleration of the particles away from each other is approximately

$$\langle a_r \rangle \sim \frac{u}{r/u} = \frac{u^2}{r}.$$

Since a shock occurs only if the particles are approaching each other, i.e. if $u_r = \dot{r} < 0$, whereas no shock is generated if $u_r > 0$, the average repulsive acceleration due to the propagation of shocks between neighboring particles is

$$\langle a_r \rangle \sim \begin{cases} u_r^2/r, & u_r < 0, \\ 0, & u_r > 0. \end{cases} \tag{3}$$

This result is identical in form to the standard artificial-viscosity term used to represent shocks in finite-difference methods [6], and it has a similar effect of spreading out the dissipation associated with shock fronts over a region with dimensions comarable to the particle separation. The use of an artificial viscosity of the form (3) corresponds to assuming a characteristic distance for momentum transfer which is comparable to the particle separation, so that it would also be appropriate for other sources of viscosity such as turbulent viscosity if the turbulent mixing length were of this order.

Combining Eq. (2) for the pressure and Eq. (3) for the viscosity acting between neighboring particles, the total repulsive acceleration is

$$a_r = \begin{cases} (C^2 + Qu_r^2)/r, & u_r < 0, \\ C^2/r, & u_r > 0, \end{cases} \tag{4}$$

where Q is a constant of order unity. The value of Q cannot be too small, since then there is not enough viscosity to dissipate the collapse energy within a free-fall time, and formation of bound condensations does not occur; instead the system behaves more like a classical n-body system. Reasonable results are obtained with $0.25 \lesssim Q \lesssim 1.0$, and most of the calculations have been made with $Q = 0.5$.

(c) *The Choice of Interacting Neighbors*

An important aspect of the finite-particle method is that it is necessary at each step to locate the nearest neighbors of each particle and decide which ones to include in calculating the total force on the particle. The simplest possibility, and the one that has been used in most of the calculations, is to include only the nearest neighbor of each particle, together with any other particles of which it is the nearest neigbor. The average number of neighbors with which a particle interacts at any instant is then typically about 1.5 to 1.6. The forces on the particles vary discontinuously whenever they change nearest neighbors, and therefore the particles are jostled around and acquire random velocities that contribute to the total pressure and viscosity of the system. However, the dissipation term in Eq. (4) acts to damp the random velocities and keep them generally smaller than the sound speed, so that the random-motion component of the pressure is usually smaller than that due to the repulsive forces.

Since there is no direct control over the random-motion contribution to the pressure and viscosity, it is desirable to reduce the random velocities as much as possible if the

method is to simulate accurately a gas with specified properties. The random velocities can be reduced by including more interacting neighbors per particle, thereby reducing the fluctuations in the force per particle. The use of more interacting neighbors may also in some circumstances increase the accuracy with which pressure gradients are represented. A scheme has therefore been tried in which neighbors are successively added such that the $(n + 1)$th interacting neighbor is the nearest particle whose direction is not within 60° of the direction to any of the previous n neighbors, until a maximum distance equal to twice that of the nearest neighbor is reached. This results in an average of about 4.5 to 5.0 interacting neighbors distributed roughly uniformly about each particle.

Increasing the number of interacting neighbors in this way is found to make no large difference to any of the results, once the value of C in Eq. (4) is reduced to give the same total pressure as before. The random velocities are reduced, as expected, and the balance between pressure and gravity is somewhat more accurately calculated for small numbers of particles. However, there are also some disadvantages, including a greater tendency for the particles to concentrate near any boundary that may be placed around the system; also, the ratio of pressure to gravity forces between neighboring particles is smaller, so that spurious two-body gravitational effects may be more important.

(d) *Gravitational Forces*

Gravitational forces have been calculated individually for all pairs of particles, as in standard n-body techniques. Computational economies have been achieved by recalculating different force components with different time steps, as described in Section 3(b). In order to alleviate possible numerical problems associated with very close encounters, and to allow for a finite size of the particles, a softened force law of the form

$$F_{12} = \frac{Gm_1m_2}{r_{12}^2 + \epsilon^2} \tag{5}$$

has been assumed in most of the calculations. However, the use of a finite ϵ (typically $\approx 1\,\%$ of the radius of the system) makes no essential difference to the results, serving mainly to slow down the rate of gravitational processes in the close vicinity of accreting condensations.

3. Numerical Features of the Method

(a) *Integration of the Particle Orbits*

Because of the discontinuously varying particle accelerations, the relatively sophisticated high-order integration schemes normally used in n-body calculations are not advantageous, and a simpler integration scheme with shorter time steps is more appropriate. We have used the "modified Euler method" which involves calculating

the forces on the particles at the beginning of each time step, extrapolating the positions and velocities to the end of the step, recalculating the forces, and then advancing all quantities using the average of the initial and final forces. The error of integration after a fixed time interval is theoretically proportional to the square of the time step, and tests have verified that this is the case with this method, despite the discontinuities in the accelerations.

From previous work on the n-body problem in stellar dynamics (eg. Miller [7], Standish [8]), it is known that it is meaningless to attempt to calculate exact particle orbits, since the slightest numerical error is rapidly amplified to the extent that all of the orbits become completely different. However, it appears that the overall properties of n-body systems can still be predicted with some reliability, so in calculations made with the present method it has been attempted to ensure that general features, such as the balance between pressure and gravity that determines whether a cloud collapses, are calculated with reasonable accuracy. Such features are not very sensitive to errors of integration, and it appears that the main effect of such errors is to increase the random velocities of the particles and raise the effective temperature of the system.

(b) *Force Calculation and Time Steps*

Essentially all of the computing time is taken up by the force calculation, which involves calculating the distances and gravitational forces between all pairs of particles, determining the nearest neighbors of all particles, and calculating the pressure and viscosity forces between the nearest neighbors. Thus it is advantageous to avoid repeating these calculations any more than necessary, and to use different time steps for different parts of the calculation. A hierarchy of time steps given by $\Delta t/2^n$ with $0 \leqslant n \leqslant 5$ has been used, and each particle has been assigned a value of n such that the corresponding time step is approximately proportional to the distance of its nearest neighbor, but is reduced if the relative velocity is particularly large. Thus particles experiencing close encounters with neighbors are advanced with short time steps, while those that are far from other particles are advanced with longer time steps. (A similar hierarchy of time steps was used by Hayli [9].) In addition, each *pair* of particles is assigned a value of n in the same way, and the distances and forces between particles are recalculated with time steps that are short for close pairs and long for distant pairs, even if the individual particles are being advanced on shorter time steps. With these economies, it is possible to follow the evolution of systems of $\sim$100 to 200 particles with moderate amounts of computing time; for example, a system of 150 particles can be followed for a time 50 Δt or $\sim$4 free-fall times in about 15 min on an IBM 370/158.

4. Tests of the Method

(a) *Pressure of a Static System*

The total pressure of a system of particles interacting according to the force law (4) can be determined experimentally by enclosing the system within a reflecting boundary

and measuring the pressure on the boundary. The measured pressure can then be compared with the predicted pressure to obtain an idea of the accuracy with which the method is capable of simulating a given temperature and pressure. In the Appendix, the predicted pressure is shown to be

$$\frac{P}{\rho} \equiv c^2 = \frac{\langle n \rangle}{6} C^2 + \left(1 + \frac{\langle n \rangle}{12} Q\right) \langle u_x^2 \rangle, \tag{6}$$

where $\langle n \rangle$ is the average number of interacting neighbors per particle and u_x is the random velocity in one coordinate direction.

When the system is enclosed in a reflecting boundary, the particles tend to concentrate near the boundary because of their mutual repulsion. This effect becomes more pronounced for smaller random velocities, but can be partially alleviated by introducing a repulsive force between the boundary and the particles closest to it. In either case, the total pressure exerted on the boundary is found to agree well with Eq. (6) if the mean density ρ and the empirical mean values of $\langle n \rangle$ and $\langle u_x^2 \rangle$ are used; the agreement is typically within 5 % for a system of 100 particles. If $Q = 1$ in Eq. (4), the fraction of the total pressure due to random motions is about 0.30 for $\langle n \rangle = 1.6$ and 0.15 for $\langle n \rangle = 5.0$; if $Q = 0$, these numbers are larger by about a factor of 2. The agreement between theoretical and measured pressures is hardly altered if different time steps are used, but numerical noise causes the relative importance of random motions to increase as the time step is increased.

(b) *Radial Oscillations of a Bounded Sphere*

The ability of the finite-particle scheme to simulate acoustic oscillations can be tested by studying the radial oscillations of a system of particles enclosed in a reflecting sphere, and comparing the observed period with that predicted by the classical theory of oscillating gas spheres. Such oscillations are set up naturally because the mutual repulsion of the particles causes the system to begin expanding initially, until the particles start colliding with the boundary. The oscillations are strongly damped by the dissipation term in Eq. (4), so for this test Q has been set equal to zero. (Setting $Q = 0$ also increases the random velocities and reduces the tendency for particles to concentrate near the boundary.)

Some results are illustrated in Fig. 3, which shows the mean radius $\langle r \rangle$ of the particles as a function of time for several runs with different numbers of particles. For $N = 50$ the oscillation is fortuitously nearly a pure fundamental mode, while for $N = 75$ and $N = 100$, higher harmonics are also evident; in all cases, however, the fundamental is sufficiently dominant that its period can be determined with reasonable accuracy, and these periods are indicated in Fig. 3. Also indicated for comparison is the theoretical period [10]

$$T = 1.398\, R/c,$$

where R is the radius of the sphere and c is the isothermal sound speed as given by

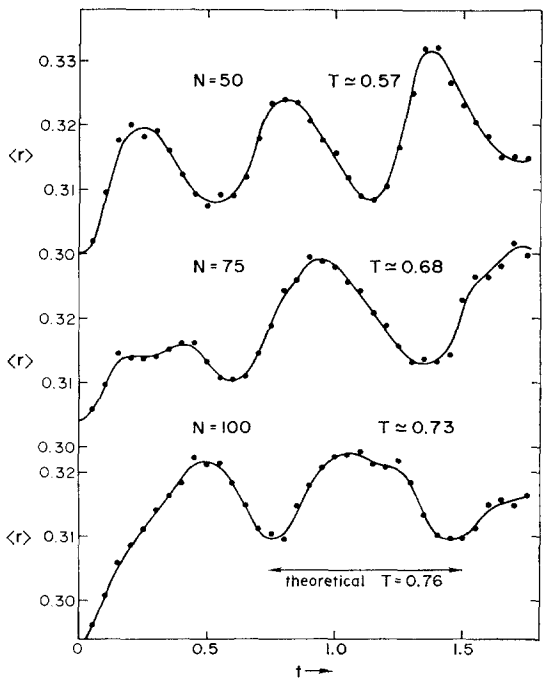

FIG. 3. Radial oscillations of systems of $N = 50$, 75, and 100 particles enclosed in reflecting spheres of radius $R = 0.4$. The mean radius $\langle r \rangle$ of all particles is plotted vs time for each case; also indicated are the observed period T of the fundamental mode in each case, and the theoretical period $T = 1.398\ R/c$.

Eq. (6). The agreement between measured and theoretical periods improves with increasing N, and approaches $\approx 5\%$ for $N = 100$. Thus the scheme appears to simulate correctly not only the static pressure but also the radial oscillations of an enclosed gas sphere.

(c) *Spherical Isothermal Collapse*

We consider next some calculations including gravitational forces, which have so far been omitted. A convenient test problem is the isothermal collapse of a sphere with a fixed boundary; this problem has been studied by several authors (eg. Bodenheimer and Sweigart [11], Larson [12]), and well-determined solutions obtained with standard Eulerian and Lagrangian methods are available. Both the density distribution resulting from the collapse and the critical temperature required to prevent collapse can be compared with the previous results to obtain an idea of how accurately the present scheme can simulate the balance between pressure and gravity and the dynamics of gravitational collapse.

The results of many such calculations show qualitatively the same behavior as found in previous studies: for temperatures above a critical value the system does not

collapse but rebounds and oscillates, while for lower temperatures the cloud continues to collapse indefinitely and develops a centrally condensed structure with a density distribution approximating $\rho \propto r^{-2}$. Some density distributions obtained for collapsing systems with temperatures slightly less than the critical value are shown in Fig. 4. The radius r is measured from the point of maximum density, which may not coincide exactly with the center of the system, and the average densities of particles are plotted for a series of concentric shells centered at this point. Also shown for comparison (solid curves) are the density distributions obtained from previous isothermal collapse calculations made with Lagrangian and Eulerian grid methods [12]. The agreement is

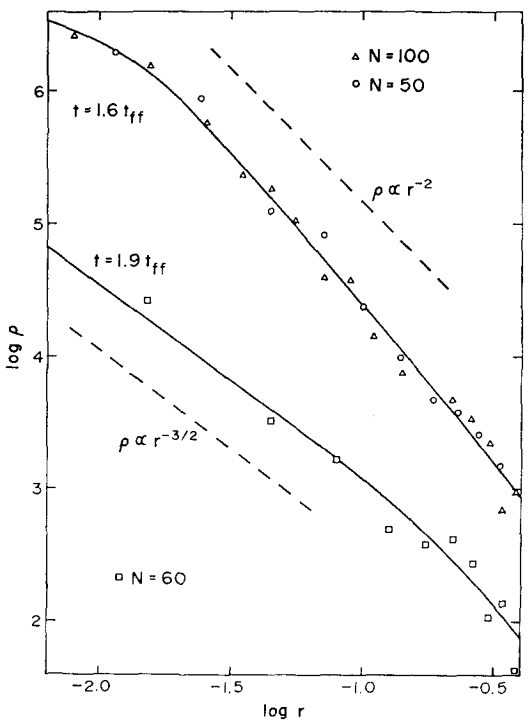

FIG. 4. A comparison of density distributions obtained with the finite-particle scheme (various symbols) and with an accurate Lagrangian grid method (solid curves) for the spherical isothermal collapse problem. Results are shown after 1.6 free-fall times (t_{ff}), just before the formation of a dense core, and at $t = 1.9\ t_{ff}$ when 40 percent of the mass has fallen into the core; the latter case is shifted downward by 1 unit in $\log \rho$ for clarity. The analytic approximations $\rho \propto r^{-2}$ and $\rho \propto r^{-3/2}$ are also shown for comparison.

evidently quite close, even with only 50 particles. Although the density distribution becomes difficult to define, qualitatively similar results are obtained with as few as 10 particles; the formation of a dense central core is still quite evident, even though it contains only a few particles. This suggests that the method is capable of following the

formation of small condensations in at least a qualitatively correct fashion even if they contain only a small number of particles.

A quantitative check on the accuracy of the method can be made by comparing the minimum value of c^2 required to prevent collapse with the critical value $c^2 = 0.46$ GM/R determined previously [12] using an accurate Lagrangian grid method. A precise comparison is difficult because of the complicating boundary effects, but the results of many calculations with different detailed assumptions can be summarized by saying that the minimum value of c^2 required to prevent collapse is smaller than the "theoretical" critical value by a factor which is about 0.6 for $N = 25$, 0.7 for $N = 50$, and 0.8 for $N = 100$; an analytic approximation for this error factor is $\sim(1 + 5N^{-2/3})^{-1}$. It is plausible that the fractional error should vary as $N^{-2/3}$ since $N^{-2/3}$ is proportional to the square of the ratio of particle separation to system size, and the error of a conventional Lagrangian scheme is also proportional to this quantity. For $N \gtrsim 50$ the error does not appear to depend much on $\langle n \rangle$, but for smaller numbers of particles there is a tendency for the error to be smaller for larger $\langle n \rangle$.

(d) *Accretion Disks*

A final test problem against which results calculated with the present method can be compared is the case of a massless isothermal accretion disk orbiting around a central point mass. The vertical density distribution in such a disk has the simple analytic form

$$\rho(z) = \rho(0) \exp(-GMz^2/2c^2r^3),$$

and the mean height $\langle z \rangle$ of matter at radius r is

$$\langle z \rangle = (2/\pi GM)^{1/2} cr^{3/2}, \tag{7}$$

where M is the central mass. The formation of an accretion disk has been simulated by calculating the collapse of a spherical, rotating system of 100 massless particles surrounding a central point mass which absorbs any particles that come closer to it than 5% of the initial radius. Nearly half of the particles are then accreted by the central mass during the initial collapse, and the rest form a flattened disk orbiting around it whose thickness depends on the assumed value of C^2 in Eq. (4). The mean height $\langle z \rangle$ of particles from the central plane of the disk increases with radius in approximate agreement with Eq. (7); an example is shown in Fig. 5.

Since most of the pressure is in this case due to random motions rather than repulsive forces, the comparison between observed and predicted values of $\langle z \rangle$ is not a strong test of the ability of the force law (2) to simulate the pressure of a gas; instead, the thickness of the disc is mainly a measure of the ability of the dissipation term in (4) to dissipate enough energy during the collapse to allow the formation of a thin disk with small random motions. With $N \sim 50$ particles in the disk, the smallest

disk height $\langle z \rangle$ obtained even with C^2 set equal to zero is approximately $0.1r$, indicating that there is a minimum attainable random velocity which is of the order of 10% of the circular velocity. This is similar to the result found by Brahic [3] using a colliding particle scheme. The disk thickness depends somewhat on the value of Q in Eq. (4), being smallest for $0.5 \lesssim Q \lesssim 1.0$ and larger for other values.

Because of the finite viscosity, angular momentum is transferred outward in the disk, causing the inner part to spiral inward and accrete onto the central object while the outer part expands, as in the viscous disk models of Lynden-Bell and Pringle [13]. The timescale for evolution of a viscous disk with kinematic viscosity ν is given by $\tau \sim \mathscr{R}\omega^{-1}$, where ω is the angular velocity of rotation and $\mathscr{R} = \omega r^2/\nu$ is the Reynolds number or ratio of inertial to viscous forces. The effective Reynolds number of the disks simulated with the present scheme can therefore be estimated from the rate at

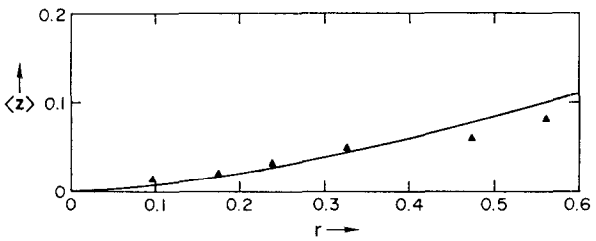

FIG. 5. The mean height $\langle z \rangle$ of particles above the plane of an accretion disc containing ~50 particles is plotted vs radius (triangles) and compared with the theoretical relation for an isothermal disk (curve).

which disk matter spirals inward and is accreted by the central object. For disks containing ~50 particles the effective Reynolds number estimated in this way is $\mathscr{R} \approx 30 - 50$, and the corresponding timescale for spiraling in and accretion of the inner parts of the disk is of the order of 5 to 8 orbital periods. This empirical Reynolds number is in approximate agreement with that predicted by the classical formula for molecular viscosity, i.e. $\nu = \frac{1}{3}\langle v \rangle \lambda$, if $\langle v \rangle$ is taken as the average random velocity of the particles and λ is taken as the mean interparticle distance. The approximate correspondence between the classical mean free path and the interparticle spacing exists because of the dissipation term in Eq. (4), which implies a path length for momentum transfer which is comparable to the particle spacing. If Q is set equal to zero, the viscosity of the disk becomes unmeasurably small.

5. CONCLUDING REMARKS

The method which has been described appears to simulate three-dimensional isothermal gas dynamics well when subjected to a number of tests. Both the static pressure and the period of radial oscillation of an enclosed gas sphere are reproduced quite closely, with an error of the order of 5% for 100 particles, if accurate empirical

values of $\langle n \rangle$ and $\langle u_x^2 \rangle$ are used in Eq. (6) to obtain the predicted pressure. In this situation at least two-thirds of the total pressure is due to repulsive forces and less than one-third to the random motions. In gravitationally collapsing systems the random motions become more important, providing perhaps about one-half of the total pressure, and the accuracy of comparisons with standard test problems is somewhat less, i.e. of the order of 20% for 100 particles. This is in part because only a fraction of the particles are in the dense collapsing core of the cloud, but also because the values of $\langle n \rangle$ and $\langle u_x^2 \rangle$ are altered during the collapse and therefore are not as well determined as in the static case. Nevertheless this level of accuracy is still very useful for many problems for which three-dimensional calculations have not previously been possible.

The major uncertainty affecting results obtained with this method arises from the assumed viscosity and the question of whether it is physically realistic. The presence of dissipation with a scale length smaller than the size of the system is essential if the method is to simulate collapse and star formation processes at all, and in the present scheme the dissipation length has been assumed to be comparable with the mean interparticle spacing. This results in a Reynolds number, or ratio of inertial to viscous forces, which is of the order of 50 for systems of 100 particles. This is about 20 times smaller than the value $\mathscr{R} \approx 10^3$ suggested by Lynden-Bell and Pringle [13] for turbulent accretion disks, but it is likely that in collapsing clouds the various additional sources of viscosity [1] make the Reynolds number much smaller than $\mathscr{R} \approx 10^3$, in which case results obtained with the present method may not be grossly in error.

APPENDIX: CALCULATION OF THE PRESSURE

We assume that particles of mass m are uniformly distributed in space with density N particles per unit volume, and that a repulsive force mC^2/r acts between each particle and its nearest neighbor. Let $f(r)$ denote the normalized distribution of nearest-neighbor separations, so that $f(r)\,dr$ is the probability that the nearest neighbor lies in the distance interval dr. Consider first the total x-component of the forces acting per unit area across the plane $x = 0$ between particles with $x < 0$ and nearest neigbors with $x > 0$. If the nearest neighbor of a particle with $x = x_1 < 0$ lies at distance r and direction θ measured from the $+x$ direction, the pair straddles the plane $x = 0$ only if $0 < \theta < \pi/2$ and $r > |x_1| \sec\theta$; the x-component of the force is then $mC^2 \cos\theta/r$. The number of particles per unit area with x_1 in the interval dx is $N dx$, and for each such particle the probability that its nearest neighbor lies in the distance interval dr and the direction interval $d\theta$ is $\frac{1}{2} \sin\theta\, d\theta\, f(r)\, dr$. Hence the total x-component of force acting per unit area across the plane $x = 0$ is

$$P_x = \int_{-\infty}^{0} N\,dx \int_0^{\pi/2} \frac{1}{2} \sin\theta\, d\theta \int_{|x|\sec\theta}^{\infty} f(r)\, dr\, \frac{mC^2 \cos\theta}{r},$$

which yields

$$P_x = \tfrac{1}{6} NmC^2 = \tfrac{1}{6}\rho C^2$$

independent of the form of $f(r)$. This derivation has so far assumed only a single interacting neighbor per particle, but since the result does not depend on $f(r)$, each interacting neighbor provides the same contribution to the total pressure. Therefore the total pressure P_C due to the repulsive forces is obtained by multiplying by the average number $\langle n \rangle$ of interacting neighbors per particle:

$$P_C = (\langle n \rangle / 6)\, \rho C^2.$$

An additional contribution to the pressure comes from the second term Qu_r^2/r in Eq. (4), representing viscosity. If the velocities of the interacting particles were uncorrelated we would have $\langle u_r^2 \rangle = 2\langle u_x^2 \rangle$, where u_x is the x-component of random velocity of a single particle; however, the interaction tends to reduce $\langle u_r^2 \rangle$ for approaching particles to approximately $\langle u_x^2 \rangle$. Multiplying by another factor of $\frac{1}{2}$ because the viscous force is zero when $u_r > 0$, the resulting contribution P_Q to the pressure is

$$P_Q = (\langle n \rangle / 12)\, \rho Q \langle u_x^2 \rangle.$$

Finally, there is a contribution to the pressure of $\rho\langle u_x^2 \rangle$ due to momentum transfer by the random motions, just as in classical kinetic theory. Hence the total pressure is

$$\frac{P}{\rho} = \frac{\langle n \rangle}{6} C^2 + \left(1 + \frac{\langle n \rangle}{12} Q\right) \langle u_x^2 \rangle.$$

REFERENCES

1. R. B. LARSON, Collapse dynamics and collapse models, *in* "Star Formation," IAU Symposium No. 75 (T. de Jong and A. Maeder, Eds.), p. 249, Reidel, Dordrecht/Boston, 1977.
2. A. BRAHIC, *J. Comput. Phys.* **22** (1976), 171.
3. A. BRAHIC, *Astron. Astrophys.* **54** (1977), 895.
4. J. R. DORMAND AND M. M. WOOLFSON, *Mon. Notic. Roy. Astron. Soc.* **151** (1971), 307.
5. C. AUST, *in* "Recent Advances in Dynamical Astronomy" (B. D. Tapley and V. Szebehely, Eds.), p. 222, Reidel, Dordrecht/Boston, 1973.
6. R. D. RICHTMYER AND K. W. MORTON, "Difference Methods for Initial-Value Problems," Wiley–Interscience, New York, 1967.
7. R. H. MILLER, *Astrophys. J.* **140** (1964), 250.
8. E. M. STANDISH, Ph.D. Thesis, Yale University (1968).
9. A. HAYLI, *Bull. Astron. Ser. 3* **2** (1967), 67.
10. J. W. S. RAYLEIGH, "The Theory of Sound," Vol. II, p. 264, reprinted by Dover, New York, 1945.
11. P. BODENHEIMER AND A. SWEIGART, *Astrophys. J.* **152** (1968), 515.
12. R. B. LARSON, *Mon. Notic. Roy. Astron. Soc.* **145** (1969), 271.
13. D. LYNDEN-BELL AND J. E. PRINGLE, *Mon. Notic. Roy. Astron. Soc.* **168** (1974), 603.
14. R. B. LARSON, Calculations of three-dimensional collapse and fragmentation, *Mon. Notic. Roy. Astron. Soc.* **183** (1978), in press.